Contents lists available at SciVerse ScienceDirect

## Physics Letters A

www.elsevier.com/locate/pla



# First-principles study of the electronic transport properties in $(GaAs)_n$ (n = 2-4) nanocluster-based molecular junctions



Daoli Zhang a,b,\*, Yuanlan Xu a, Jianbing Zhang a,b, Xiangshui Miao a,b

- <sup>a</sup> School of Optical and Electronic Information, Huazhong University of Science and Technology, 1037 Luoyu Road, Hongshan District, Wuhan City, Hubei Province, 430074, PR China
- <sup>b</sup> Wuhan National Laboratory for Optoelectronics, 1037 Luoyu Road, Hongshan District, Wuhan City, Hubei Province, 430074, PR China

#### ARTICLE INFO

Article history:
Received 5 July 2012
Received in revised form 5 September 2012
Accepted 18 September 2012
Available online 24 September 2012
Communicated by R. Wu

Keywords: GaAs nanocluster Molecular device Negative differential resistance

#### ABSTRACT

In this program the geometric structures and electronic transport properties of a series of  $(GaAs)_n$  (n=2,3,4) clusters are comparatively studied using non-equilibrium Green's function (NEGF) combined with density functional theory (DFT). It is find that all the GaAs nanocluster-based molecular junctions show metallic behavior at low biases ( $[-2\ V,2\ V]$ ) while negative differential resistance (NDR) appears at a certain high bias range. Our calculation shows that the current of  $(GaAs)_3$  nanocluster-based molecular junction is almost the smallest at any bias. The mechanisms of the current-voltage characteristics of all the three molecular junctions are proposed.

© 2012 Elsevier B.V. All rights reserved.

#### 1. Introduction

In recent years, molecular devices have attracted much attention for many interesting physical properties have been found in these devices, such as NDR [1], single-electron characteristics [2], Coulomb blockade [3], current rectification [4], electrical switching [5], and so on. However, most of the molecular devices reported to date are based on small organic molecules [6,7], C<sub>60</sub> [1,8], graphite [9,10] or these materials with some modifications [5,11,12]. Very few works have attempted to study the transport properties of junctions based on inorganic clusters, such as GaAs.

As one of the most important inorganic semiconductors, GaAs materials have attracted a widespread interest due to their large potential applications including solar cells [13], optoelectronic sensors [14], in vivo imaging for medical diagnostics [15], nonlinear optics [16] and quantum computing [17]. Much progress has also been made in the theoretical study of GaAs clusters in the past decade. Feng et al. [18] studied the structure of  $Ga_nAs_m$  clusters for  $n + m \le 16$ . Gutsev et al. computed the structure of  $(GaAs)_n$  clusters for n = 2-40 and their positively and negatively charged ions for n = 2-15 [19–21]. They also studied the optical properties of

E-mail address: zhang\_daoli@mail.hust.edu.cn (D. Zhang).

 $(GaAs)_n$  (n=2-16) and reported the results of gap between Lowest Unoccupied Molecular Orbital (LUMO) and Highest Occupied Molecular Orbital (HOMO), the excitation energies and oscillator strengths [20]. Jiang et al. studied the energy band gap of GaAs nanoclusters with diameter ranging from 2.6 to 16.7 nm [22]. In experiment, photoionization [23] and photoabsorbtion spectra [24] of GaAs nanoclusters were studied. However, as far as we know, no investigation focusing on their electronic transport properties has been reported.

In this work, we investigate the electronic transport properties in  $(GaAs)_n$  (n=2-4) nanocluster-based molecular junctions. Interestingly, the inorganic  $(GaAs)_n$  nanocluster-based molecular junctions studied here also display some properties obtained in organic molecular devices.

#### 2. Geometric structure and computational method

The structures of  $(GaAs)_n$  (n=2-4) nanoclusters were optimized and showed in Fig. 1. The geometric configuration of  $(GaAs)_2$  is rhombi which is just as found in previous studies [18, 19]. The geometry of  $(GaAs)_3$  is a bridged trigonal bipyramid, which agrees well with previously reported result [25]. The optimized structure of  $(GaAs)_4$  is parallelepiped formed from  $Ga_2$  and  $As_2$  dimers which was first found by Gutsev et al. [19]. It should be noted that the geometric configuration parameters including bond angles and bond lengths vary a little from method to method within reasonable range due to different calculation methods.

<sup>\*</sup> Corresponding author at: School of Optical and Electronic Information, Huazhong University of Science and Technology, 1037 Luoyu Road, Hongshan District, Wuhan City, Hubei Province, 430074, PR China. Tel.: +86 27 8754 2894; fax: +86 27 8754 2693.

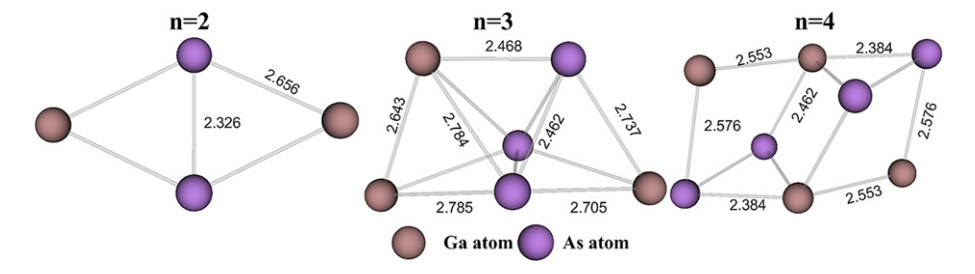


**Fig. 1.** Optimized structures of  $(GaAs)_n$  clusters for n = 2-4. Bond lengths are in Å.

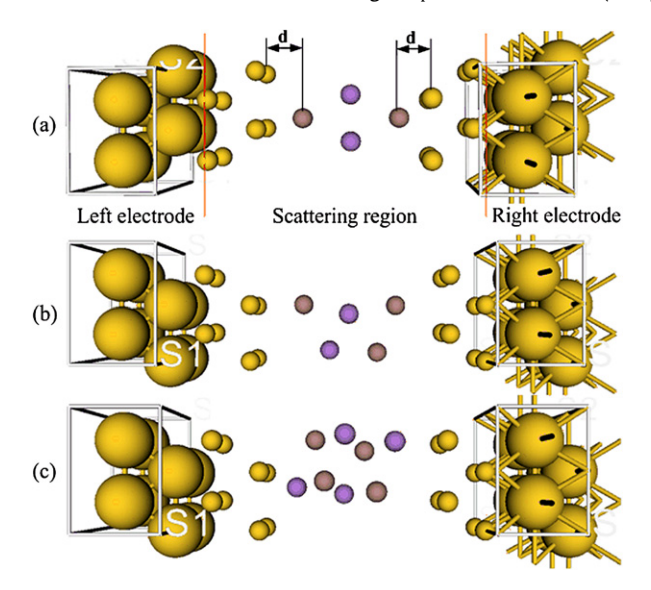


**Fig. 2.** Schematic plot of  $(GaAs)_n$  molecular junction for: (a) n=2, (b) n=3 and (c) n=4. The junction consists of three regions. The extended region consists of molecule  $2 \times 2$  (001) two layers of Au slab in the left electrode and two layers of Au slab in the right electrode, between which is the scattering region. d is the left and right axial distance. M1, M2, and M3 denote  $(GaAs)_2$ ,  $(GaAs)_3$  and  $(GaAs)_4$ -based junction, respectively.

The quantum transport properties in the  $(GaAs)_n$  (n = 2-4)nanocluster-based molecular junctions are calculated with the ATK package [26,27]. The configurations studied here are illustrated in Fig. 2, which are divided into three regions: the left electrode, the central scattering region and the right electrode. The scattering region includes the GaAs nanocluster and a portion of the semiinfinite electrodes to screen the interaction between GaAs clusters and the electrodes. The extended region consists of molecule  $2 \times 2$ (001) two layers of Au slab in the left electrode as well as two layers in the right electrode. The GaAs clusters are so small that a  $2 \times 2$  layers in x and y directions is large enough. However, eight layers [28] of Au slab were chosen in z direction and then they decrease to five layers [4,8,29] in some current studies for a fast computational speed. In this work, only four layers of Au slab are used because they are enough for such small clusters. The perpendicular distance between the left electrode and the leftmost atom of the cluster as well as counterpart in the right is 2.0 Å which is a typical distance in the interface between electrode and molecule [30]. We keep all gold atoms fixed and relax the cluster in the center until the forces on each atom are smaller than 0.05 eV/Å in the optimization.

In our simulations, Perdew–Burke–Ernzerhof version of the generalized gradient approximation (GGA.PBE) is used [31]. Valence electrons are expanded in a single- $\xi$  along with polarization basis set (SZP) for Au atoms and a double- $\xi$  along with polarization basis set (DZP) for other atoms.

The Brillouin zone is set to be  $5 \times 5 \times 100$  points following the Monkhorst-Pack k-point scheme. The cut-off energy and the iter-

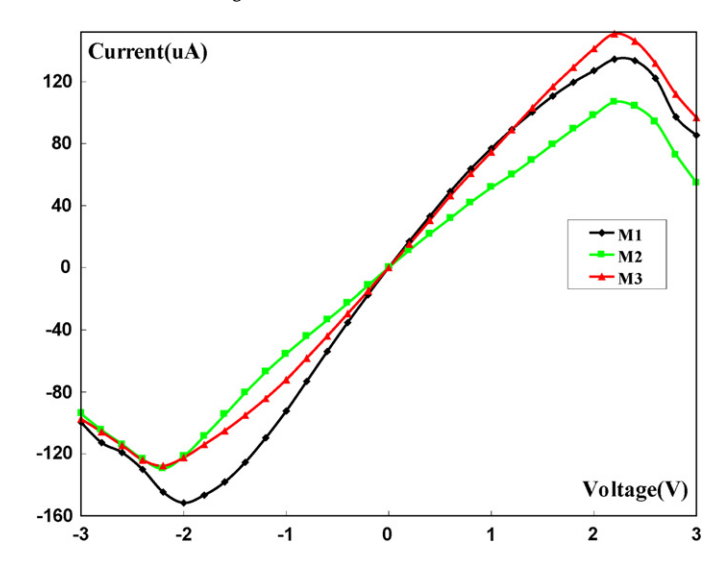


**Fig. 3.** The I-V characteristic curves of the GaAs cluster-based junctions.

ated convergence criterion for total energy are set to 150 Rydberg and  $10^{-5}$ , respectively. M1, M2, and M3 denote junctions based on (GaAs)<sub>2</sub>, (GaAs)<sub>3</sub> and (GaAs)<sub>4</sub> cluster, respectively.

#### 3. Results and discussion

In Fig. 3, we show the I-V curves of all three systems M1, M2 and M3 with the bias voltages in the range from -3.0 V to 3.0 V in steps of 0.2 V. We note that the current is obtained self-consistently under non-equilibrium conditions at each bias voltage. In NEGF theory, the I-V characteristics are determined by the Landauer-Bütiker formula [32]:

$$I(V) = \frac{2e}{h} \int_{\mu_L}^{\mu_R} [f(E - \mu_L) - f(E - \mu_R)T(E, V)] dE$$
 (1)

where e is the electron charge, f the Fermi function, h Planck's constant, T(E,V) the transmission function of the system, and  $\mu_R$  as well as  $\mu_L$  the electrochemical potential of the right and left electrodes, respectively,  $\mu_R = E_F - eV/2$  and  $\mu_L = E_F + eV/2$ . The Fermi level of the system  $E_F$  is set to be zero in all the calculations. The transmission function T(E,V) of the system is the sum of the transmission probabilities of all channels available at energy E under external bias voltage V [32]

$$T(E, V) = T_r \left[ \Gamma_L(V) G^R(E, V) \Gamma_R(V) G^A(E, V) \right]$$
 (2)

where coupling functions  $\Gamma_L$  and  $\Gamma_R$  are the imaginary parts of the left and right self-energies,  $G^R$  and  $G^A$  are the retarded and advanced Green's functions, respectively.

From Fig. 3, we can see that all three nanocluster-based junctions show the metal characteristics, with a linear region from  $-2.0~\rm V$  to  $2.0~\rm V$ . This is due to the interaction between the clusters and the metal electrodes, resulting in electrons of metal doped

### Download English Version:

# https://daneshyari.com/en/article/10727515

Download Persian Version:

https://daneshyari.com/article/10727515

<u>Daneshyari.com</u>